Polymer Journal, Vol. 14, No. 6, pp 441—456 (1982)

Thermal Behavior of *n*-Alkanes from *n*-$C_{32}H_{66}$ to *n*-$C_{80}H_{162}$, Synthesized with Attention Paid to High Purity

Kanichiro TAKAMIZAWA, Yoshihiro OGAWA,* and Tomo-o OYAMA

Department of Applied Science, Faculty of Engineering, Kyushu University, Hakozaki, Higashi-ku, Fukuoka 812, Japan.

(Received October 7, 1981)

ABSTRACT: The general principle for synthesizing higher *n*-alkanes of the highest purity is described briefly. Thermal behavior of the synthesized *n*-alkanes from *n*-$C_{32}H_{66}$ to *n*-$C_{80}H_{162}$ were examined by means of DSC, small- and wide-angle X-ray scattering and optical microscopy. All the crystalline *n*-alkanes except for *n*-$C_{80}H_{162}$, when crystallized from solution, showed transitions to high-temperature monoclinic modifications (M_{h01}, $h=1$ or 2) before the rotator transition or the melting, irrespective of the number of carbon atoms (n) being odd or even and the difference in room-temperature modifications of even *n*-alkane. One feature of the transition was its irreversibility. The odd *n*-alkanes of *n*-$C_{33}H_{68}$, *n*-$C_{37}H_{76}$, and *n*-$C_{45}H_{92}$ showed also another type of solid-solid transition below the transition mentioned above. Both types of the transitions were thermally proved to be of the first-order. Although no simple functional forms were generally given to the relationships between the transition temperature and n, the temperatures for the transition of orthorhombic higher *n*-alkanes to the M_{h01} phase increased with n, reaching about 90°C for *n*-$C_{69}H_{140}$. The transition to M_{h01} was accompanied by a morphological change on the crystal surface, in the form of characteristic striations parallel to the b_s subcell axis. This suggests that the solid-solid transition proceeds successively from a nucleating site with a staggering of molecules in the chain direction. If the slow rate of the process and complicated behavior of the M_{h01} phase are taken into account, the kinetical view point of the phase transition leads to the working hypothesis that the molecular motion of the long chains in the *n*-alkane crystals, which consists of rotational and longitudinal motions or a flip-flop motion, takes place only in this transformation process.

KEY WORDS Higher *n*-Alkanes / Synthesis / DSC / Small-Angle X-Ray Diffraction / Thermal Behaviors / Solid-Solid Phase Transition /

Crystalline *n*-alkane homologues have been studied as a simple model system to obtain insight into the thermal behavior of the polyethylene crystal in particular and polymeric crystals in general. Of particular interest is the first-order solid-solid transition observed for solution-grown crystals of heptacosane (*n*-$C_{27}H_{56}$),[1] tritriacontane (*n*-$C_{33}H_{68}$),[2] hexatriacontane (*n*-$C_{36}H_{74}$)[1,3,4] and tetratetracontane (*n*-$C_{44}H_{90}$),[3] besides (if present) a transition to a phase generally called as the rotator phase. The heat of this transition is much smaller than the heat of fusion and even than that of the rotator transition. Another feature of the transition is its irreversibility.

Transformations in the crystalline forms may be schematically described in terms of the model structures proposed by Keller[5] for crystalline *n*-alkanes. For the *n*-alkanes discussed below, four methylene groups in the two chains are considered to occupy an identical orthorhombic subcell, irrespective of the differences in modification and chain length. End methyl groups form a terminal plane indexable in terms of the subcell. These modifications can be represented by various oblique structures, including a vertical structure. The solid-solid phase transition occurs among these structures. The transformation seems to occur progressively by chain molecules slipping over each other from a nucleat-

* Present address: *Ariake Technical College, Omuta, Fukuoka 836, Japan.*

ing site while still maintaining their original orientation with the chain axis.

An increase in the intensity of small-angle X-ray scattering (SAXS) maxima with temperature, exhibited by crystalline n-$C_{36}H_{74}$, n-$C_{44}H_{90}$, and tetrananocontane (n-$C_{94}H_{190}$)[3,6] was examined in conjunction with similar behavior observed for polyethylene single crystals, which was interpreted in terms of surface melting (see ref 7 and 8 as review articles). A sharp increase in intensity as well as a change in the long period was observed at the solid-solid transition temprature.[3] On the other hand, these changes occurred for n-$C_{94}H_{190}$ with no thermal indication of the first-order transition.[6] A similar observation was reported for hexacontane (n-$C_{60}H_{122}$), heptacontane (n-$C_{70}H_{142}$), and octacontane (n-$C_{80}H_{162}$).[9] Sullivan and Weeks[6] interpreted the behavior of n-$C_{94}H_{190}$ as due to defects which cause surface vacancies in contrast to the case of the shorter n-alkanes.

Strobl *et al.* have recently carried out considerable research on the thermal behavior of higher purity n-$C_{33}H_{68}$ using a variety of experimental techniques such as wide-angle X-ray scattering (WAXS),[2] SAXS,[10] wide-line NMR,[11] IR,[11] Raman spectroscopy[12] and quasielastic neutron scattering.[13] This odd n-alkane showed four crystalline modifications, denoted as A, B, C, and D in order of increasing temperature.[2] Phase A is an orthorhombic modification common to odd n-alkanes, and D corresponds to the rotator phase. All the transitions were of the first-order. The increase in SAXS intensity and a definite decrease in the long period were observed in the transition from B to C.[10] In their study on the molecular motions of n-$C_{33}H_{68}$ these authors concerned in part with gaining an understanding of polymer chain motion in crystals, which constitutes the viscoelastic α process and surface melting and premelting phenomena. There is still dispute as to the mechanisms involved. One of the conclusions made by these authors is that the solid-solid transitions may generally be regarded as reactions of the crystal lattice at the onset of specific types of molecular motion.[14,15]

There is no relevance of the onset of the molecular motion to the solid-solid transition for n-alkanes having more than 60 carbon atoms.[6,9] Our first concern is whether generally this is actually the case. Structural changes without a definite thermal indication of the phase transition may perhaps be induced by movements or the occurrence of defects within the crystalline core.

There are two possible kinds of defects in long-chain crystals of different origins. One arises from impurities, especially homologues of different chain lengths. The other is introduced during the crystallization process, even in a sample of the highest purity. To gain a better understanding of this matter, it is desirable to differentiate the causes for defects. The effects of homologous impurities on the solid-solid transition for n-$C_{36}H_{74}$ can be found in reported data. Its monoclinic modification transforms through an intermediate phase to the rotator one. The intermediate phase has been reported to exist over a temperature range from 0.8[18] to about 6°C, while the melting point and the transition point to the rotator phase are almost constant.[1,3,4,16-19] Although purities of some samples used were not reported, it may be said that the solid-solid transition temperature is remarkably lowered, becoming less clear with an increase in impurity concentration. Thus, a sample impurity makes it very difficult to detect thermally the phase transition. This situation seems to be more serious for longer chain crystals.

Another problem is how a solid-solid transition (B→C) temperature, such as 66°C for n-$C_{33}H_{68}$,[2] depends on the number of carbon atoms. The temperatures at which structural changes take place for long n-alkanes[9] were reported to be about 70°C. These suggest that the transition temperature hardly depends on chain length if this 70°C is regarded as the transition temperature. Along with this suggestion, information regarding the motions of n-alkane crystals could be applied to the behavior of the α-process for the polyethylene crystals. Is the estimated chain length dependence reliable? If Keller's hypothesis which maintains that the slipping mechanism of chain molecules is applicable to the solid-solid transition is valid, it seems that the slipping evokes with increasing difficulty and finally ceases to exist as the chain length becomes longer when low concentration of the defects is assumed.

This work was undertaken to obtain a better understanding of the problems described above. Higher n-alkanes of the highest purity up to nonahexacontane were synthesized. We also obtained a pure n-$C_{80}H_{162}$, utilizing a preparative GPC technique, from a mixture of n-alkanes, whose

number of carbon atoms differed by 40. Methods for obtaining pure higher *n*-alkanes are given. The solid-solid transitions of the *n*-alkanes, even and odd ones, are examined by means of DSC, SAXS and WAXS. The relationship between the solid-solid transition and the chain length is presented.

EXPERIMENTAL

General Description of Sample Syntheses

In order to obtain *n*-alkanes of the highest purity, it is crucial to prevent the introduction of homologues of different chain lengths and isomers having short-branches during the process of *n*-alkane synthesis. Impurities may be introduced at each step in the synthesis: a) starting materials, b) chain extension reactions, and c) *n*-alkane synthesis. We describe here in brief our principle for the synthesis and methods of purification used.

a) Starting Materials. To obtain reactants for the final step c), alkyl alcohol and dicarboxylic acid were used as the starting materials. Long-chain compounds, whose sources are in fats and fatty oils, were suitable since they contain no branched isomers, and their homologues can be separated by fractional distillation. Also, they are inexpensive. As alkyl alcohols myristyl-(n-$C_{14}H_{29}OH$), cetyl-(n-$C_{16}H_{33}OH$) and stearyl alcohol (n-$C_{18}H_{37}OH$) were used. Azelaic ($HOOC-(CH_2)_7-COOH$), and sebacic acid ($HOOC-(CH_2)_8-COOH$) were used as dicarboxylic acids. Fractional vacuum distillation was carried out for the acetylated alcohols and dimethyl esters of the dicarboxylic acids. Fractions whose gas chromatograms (GC) showed no homologue inclusion were used as the starting material. The bromination of the purified alcohols was performed with the dry gas of hydrogen bromide. Alkyl iodide was prepared from the alcohols with iodine and red phosphorous.

b) Chain Extension Reactions. The dicarboxylic acids were chain-extended according to the method of Hünig *et al.*[20] using 1-morpholinocyclododecene.

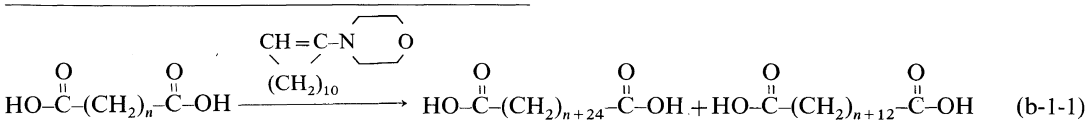

(b-1-1)

Two products of dicarboxylic acid, differring by 12 carbon atoms, were completely separated by recrystallization and extraction of their propyl esters. The purities were examined by GC. This extension reaction also can be applied to monocarboxylic acid.

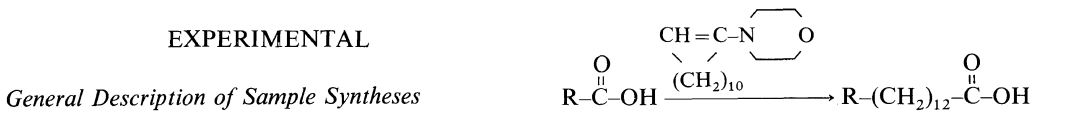

(b-1-2)

Another chain extension reaction was the Grignard reaction of alkyl bromide with carbon dioxide. This resulted in an odd-numbered carboxylic acid which was needed for synthesizing odd *n*-alkanes.

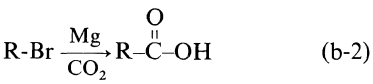

(b-2)

c) Syntheses of n-Alkanes. The well-known synthetic method of higher *n*-alkanes is the Wurtz reaction of alkyl iodide.

(c-1)

Ställberg *et al.*[21] used this method to obtain hectane, the highest synthetic *n*-alkane. A product from disproportionation can be easily removed by a treatment with hot sulfuric acid (120°C).

Another synthetic method was proposed by Reinhard and Dixon,[22] who pointed out that branching could result from side reactions of the Wurtz reaction. By this method, n-$C_{94}H_{190}$ was synthesized, and its physical properties have been throughly investigated by many American researchers. This method involves the following two steps. The first step is the Blaise–ketone synthesis (B–K) of alkyl bromide and dicarboxylic acid chloride.

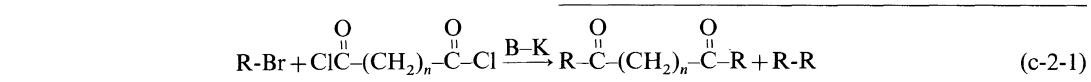

(c-2-1)

Diketone and *n*-alkane as a side-reaction product are obtained. Separation of these products was made by using their solubility difference. To enhance the separation efficiency it is desirable to use shorter alkyl bromide and longer dicarboxylic acid chloride. Reinhard–Dixon's combination for the preparation of n-$C_{94}H_{190}$ ($R = n$-$C_{42}H_{85}$- and $n = 8$) seems somewhat unreasonable. The second step is the Wolff–Kishner reduction (W–K) of purified diketone.

$$R\text{–}\overset{O}{\overset{\|}{C}}\text{–}(CH_2)_n\text{–}\overset{O}{\overset{\|}{C}}\text{–}R \xrightarrow{W\text{–}K} R\text{–}(CH_2)_n\text{–}R \qquad \text{(c-2-2)}$$

This method can also be applied to monocarboxylic acid chloride.

$$R_1\text{–}Br + Cl\text{–}\overset{O}{\overset{\|}{C}}\text{–}R_2 \xrightarrow{B\text{–}K} R_1\text{–}\overset{O}{\overset{\|}{C}}\text{–}R_2 + R_1\text{–}R_1 \qquad \text{(c-3-1)}$$

$$R_1\text{–}\overset{O}{\overset{\|}{C}}\text{–}R_2 \xrightarrow{W\text{–}K} R_1\text{–}CH_2\text{–}R_2 \qquad \text{(c-3-2)}$$

It should be noted that Reinhard–Dixon's method directly leads to odd *n*-alkanes.

Here we comment on the possibility of a branching reaction in the Wurtz synthesis. Heitz *et al.*[9,10] obtained pure n-$C_{33}H_{68}$ from a cross Wurtz reaction of n-$C_{11}H_{23}Br$ and n-$C_{22}H_{45}Br$, followed by separation by a gel-permeation chromatography (GPC). On the other hand, we synthesized a n-$C_{33}H_{68}$ sample using reaction (c-3). The samples synthesized by these two different methods gave almost identical DSC curves (see Figure 5 in ref 23). Considering the very effect of impurities on the solid-solid transition temperature, we can utilize the Wurtz reaction for the preparation of *n*-alkanes without having to take branching into consideration.

Examination of purity by GC was made using a Shimadzu GC-4B instrument equipped with a column of 1% Silicone OV-17 supported on Chromosorb W. Elution of *n*-alkanes up to octatetracontane at 290°C allowed a complete separation of the homologues. GPC examination for higher *n*-alkanes was carried out by a Shimadzu-DuPont Liquid Chromatograph 830 equipped with three HSG columns. Elution was performed at 115°C with *o*-dichlorobenzene as the solvent.

Polymerization of polymethylene diiodide by the Wurtz reaction yielded a homologous mixture of polymethylene.

$$I\text{–}(CH_2)_n\text{–}I \xrightarrow[H]{Na} H\text{–}(C_nH_{2n})_m\text{–}H \qquad \text{(c-4)}$$

Following condensation, catalytic hydrogenation was necessary to reduce the olefinic end groups and remaining iodine. This method was used first for $n = 10$ by Carothers *et al.*,[25] who separated the homologues by molecular distillation. Heitz *et al.*[9] separated the homologues of $n = 20$ by GPC. To improve the separation efficiency, a diiodide having a larger *n* is desirable because GPC resolution is still limited.

Description of Sample Syntheses

The reaction route for each *n*-alkane is briefly described, based on the methods given in the preceding paragraph. A full description is given in ref 24.

Dotriacontane (n-$C_{32}H_{66}$). This even *n*-alkane was obtained as a by-product in the B–K reactions (c-2-1) for tritriacontane or pentahexacontane (GC purity >99.9%).

Tritriacontane (n-$C_{33}H_{68}$). This was synthesized by the reaction (c-3) of cetyl bromide with heptadecanoyl chloride obtained from cetyl bromide by the reaction (b-2) (GC purity >99.9%).

Hexatriacontane (n-$C_{36}H_{74}$). A by-product in the B–K reactions for pentatetracontane or nonahexacontane (GC purity >99.9%).

Heptatriacontane (n-$C_{37}H_{76}$). From myristyl bromide and azeloyl chloride by (c-2) (GC purity >99.9%).

Pentatetracontane (n-$C_{45}H_{92}$). From stearyl bromide and azeloyl chloride by (c-2) (GC purity >99.9%).

Octatetracontane (n-$C_{48}H_{98}$). This alkane was obtained by a method different from the general scheme. Tetracosanoic acid was used as the starting material. A commercial product contained trace of docosanoic acid. The Wurtz reaction was carried out on tetracosyl iodide, obtained by the alcohol from the acid (GC purity >99.9%).

Hexacontane (n-$C_{60}H_{122}$). This compound was prepared by (c-1) from triacontyl iodide drived through (b-1-2) from stearoyl chloride.

Henhexacontane (n-$C_{61}H_{124}$) was synthesized through (c-2) from myristyl bromide and tritriacontanoyl dichloride, which had been prepared

through (b-1-1).

Pentahexacontane (n-$C_{65}H_{132}$) was made from cetyl bromide and tritriacontanoyl dichloride through (c-2).

Nonahexacontane (n-$C_{69}H_{140}$) was made from stearyl bromide and tritriacontanoyl dichloride through (c-2).

Octacontane (n-$C_{80}H_{162}$). This compound was separated by GPC from a homologous mixture of the general formula H-$[(CH_2)_{40}]_m$-H, obtained by the method (c-4). A more detailed description on the preparation is given in ref 26.

Crystallization

All the crystalline *n*-alkanes used in this study were crystallized from dilute solutions. The criterion for selecting a suitable solvent for a *n*-alkane was that the crystallization takes place at a temperature below the solid-solid transition of the *n*-alkane. The use of such a solvent prevented the introduction of structural imperfections arising from the irreversible solid-solid transition. Our solvents were pentane for n-$C_{32}H_{66}$ and n-$C_{33}H_{68}$, hexane for n-$C_{36}H_{74}$, n-$C_{37}H_{76}$, n-$C_{45}H_{92}$, and n-$C_{48}H_{98}$, and butyl acetate for n-$C_{60}H_{122}$, n-$C_{61}H_{124}$, n-$C_{65}H_{132}$, and n-$C_{69}H_{140}$, respectively. The solution concentration was about 0.1 wt%, and the cooling rate about $1°C\,h^{-1}$. The crystals were filtered and the mat obtained was dried in vacuum. It is known that according to the crystallization conditions even *n*-alkane crystallizes to an orthorhombic modification as well as a stable monoclinic one. The effect of the crystallization conditions on the modifications was examined with n-$C_{48}H_{98}$.

Measurements

DSC measurements were performed with a Perkin-Elmer DSC-1B. The standard heating rate was $5\,K\,min^{-1}$, and the sample size was from 1.0 to 1.5 mg. The transition temperature was determined from the points at which the base line intersected with the extrapolated line of a leading slope of the transition peak. Temperature calibration was made with melting temperatures of the *n*-alkanes, whose values have been compiled by Broadhurst.[17]

WAXS measurements were made using a RIGAKU diffractometer 2027, which served for transmission diffraction. A RIGAKU 2-C camera was used for the SAXS measurements. These measurements were made using Ni-filtered copper radiation. A strip 1 mm thick and 10 mm long, cut from a single crystal mat was fitted to a holder and covered with a metal block having beryllium windows and a thermostat installed. To avoid a temperature gradient within the sample, the upper and lower parts of the block were separately controlled. The temperature of the sample was maintained to within ± 0.1 K throughout the entire period of measurement.

RESULTS AND DISCUSSION

The Solid-solid Phase Transitions of Odd n-Alkanes Having from 31 to 45 Carbon Atoms

DSC curves for odd *n*-alkanes, n-$C_{33}H_{68}$, n-$C_{37}H_{76}$, and n-$C_{45}H_{92}$ indicate two small endothermic peaks due to solid-solid transitions and a rotator transition that exists except for n-$C_{45}H_{92}$. In Figure 1, the peaks due to the melting and the rotator transition are drown over-scale in order to show clearly the features of the small peak. The behavior of the solid-solid transitions for the odd *n*-alkanes over this range of chain length is thought to be common to that for n-$C_{33}H_{68}$, which has been examined in detail by Strobl *et al.*[2,10-15] The phases are denoted by A, B, C, and D in the order of

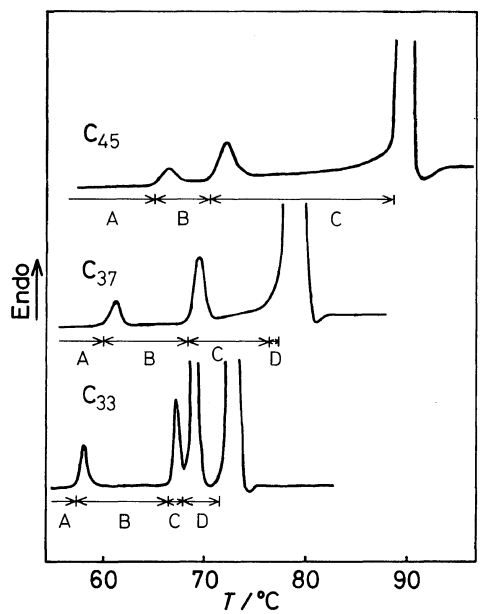

Figure 1. DSC curves of n-$C_{45}H_{92}$(C_{45}), n-$C_{37}H_{76}$(C_{37}), and n-$C_{33}H_{68}$(C_{33}) crystals. Symbol A, B, C, and D denote the phases.

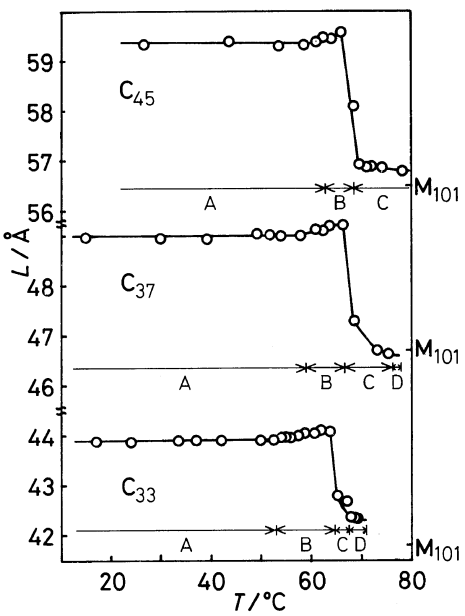

Figure 2. Temperature dependence of long periods, L, for n-$C_{45}H_{92}(C_{45})$, n-$C_{37}H_{76}(C_{37})$, and n-$C_{33}H_{68}(C_{33})$ crystals. Calculated L value corresponding to the M_{101} structure is shown on right-hand ordinate.

increasing temperature.[2] Phase A is the orthorhombic modification and phase D corresponds to the rotator modification. The A→B transition temperatures increase more rapidly than the B→C transition temperatures with increasing chain length. The heats of the A→B transitions per mole showed no dependence on chain length. Figure 2 shows the changes in the long periods, L, for the alkanes with temperature. The values for L at room temperature coincide with those calculated from the relation,

$$L = 1.273n + 1.98 \quad (\text{in Å}) \qquad (1)$$

which was proposed by Broadhurst[17] for the orthorhombic crystal of n-alkane having n carbon atoms. The A→B transition brought about a slight increase in L of from 0.1 to 0.2 Å. But, a sharp decrease in L was observed at the B→C transition temperature.

The photographs in Figure 3 show morphological changes in the n-$C_{37}H_{76}$ crystals resulting from the phase transitions. A typical crystal (Figure 3a) at room temperature is plate-like and lozenge-shaped, characteristic of an alkane crystal. Electron-microscopic observation indicated that the thickness of the plate-like crystals extended from 500 to 600 Å. The number of layers stacked up in one crystal was from 10 to 12. The transition to the B phase caused no visual change. Passing over the B→C transition temperature, fine and regular striations parallel to the b_s axis of the subcell appear on the surface of the crystal (Figure 3b). These striations were formed in the inner part of the crystal and then gradually developed outwards. The striations sometimes propagated from broken parts. The number of striations increased as shown in Figure 3c. In the temperature range of the phase D, more striations appear and become irregular (Figure 3d).

The axial length of the subcell a_s continuously changes through the modification A and B, as shown in Figure 4. As suggested by Strobl *et al.*,[10] the a_s length can be represented by a linear function of temperature over each phase region and the intersection of the two lines approximately corresponds to the A→B transition temperature. The difference in the expansion coefficients of the a_s length seems to be independent of the molecular length. This fact suggests that the WAXS measurement on higher n-alkanes is useful for detecting the A→B transition, if present, because the thermal detection is anticipated to become difficult owing to a decrease in this transition heat relative to that of the entire transition to liquid as the length of odd n-alkane increases.

Extensive studies on crystalline n-$C_{33}H_{68}$ by the German group specified defect structures for all four modifications and the corresponding molecular motions.[14,15] However, the relation between the crystal structure and the types of molecular motion is still puzzling. The result of this group on the modification B are as follows: the structure is monoclinic and its space group is A_a. Since the A→B transition induces a coupled 180° jump motion, the orientational long-range order of the zigzag plane is said to be broken down[15] at the phase B. Is there any correlation between this monoclinic form and the defect structure? The crystal structure of the phase C was determined to be monoclinic[2] and whose end plane has a $(101)_s$ subcell index. This form has been denoted as M_{101} according to the Sullivan–Weeks notation.[6] In the phase C, disorders alongside the chain axis are introduced. The superposition of "flip-flop" screw jumps, which

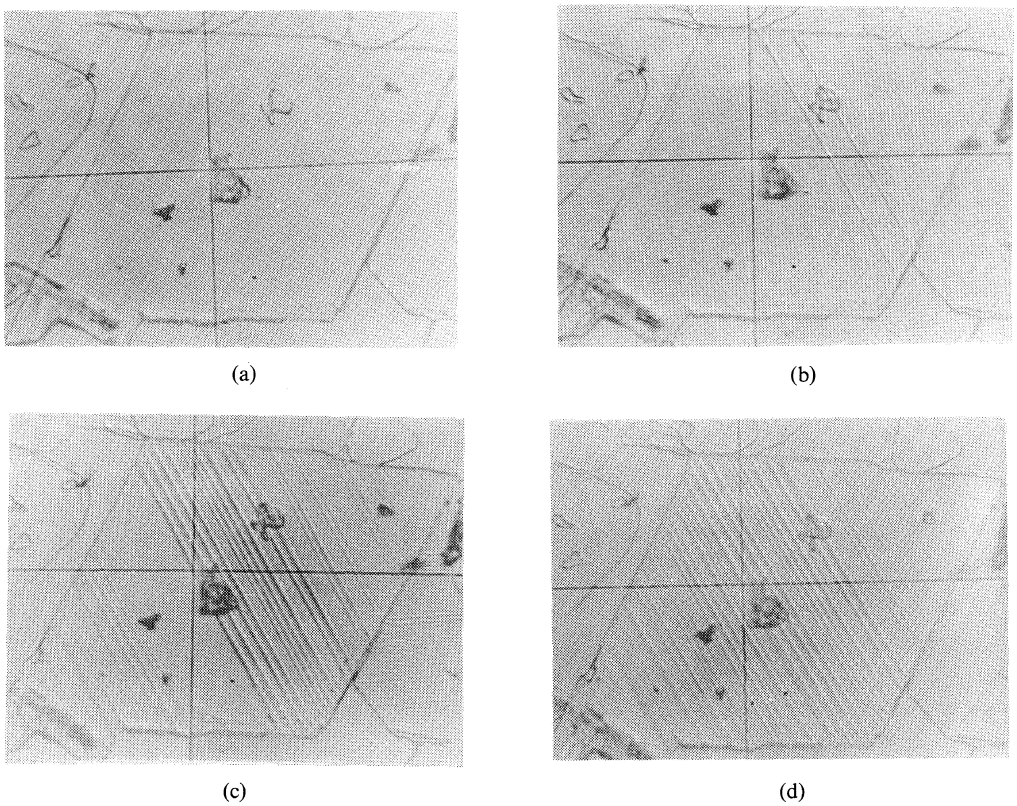

Figure 3. Photomicrographs of n-$C_{37}H_{76}$ crystal at various temperature regions: (a) at the region of the phase A; (b) at an initial stage of the region of the phase C; (c) at a higher temperature of the phase C; (d) at the region of the phase D.

were proposed by Olf and Peterlin,[29,30] onto the pure rotational jumps was first assumed.[14]

Later, the rotational and longitudinal jump motions were shown to be independent of each other.[13] Both motions were considered to take place at any site in the phase C. However, the vertical structure may be anticipated if the motions are random.

Our first concern is the relationship between the chain length and the solid-solid transition, especially the accompanying changes in the obliquity of the crystal structure. This relationship may be useful for obtaining a better understanding of the thermal behavior of polymeric crystals. Short bars on the right side in Figure 2 indicate the L values of M_{101} calculated for the respective n-alkanes. The calculation was made in the following manner: Sublattice parameters a_s and b_s at the transition temperature were evaluated from WAXS measurements. On the assumption that the end plane had a rational sublattice index and c_s was independent of temperature, the inclination angle of the molecular chain to the plane was then calculated. The L value of M_{101} was given by using the angle and L just below the transition temperature. There is uncertainty about this value in regard to the distance between the end methyl groups stacked with each other. The agreement between the calculated and the observed values shows that the phase C for the n-alkanes examined has in general the M_{101} structure.

For n-$C_{45}H_{92}$, complicated B→C transition behavior was observed. Figure 5 shows the SAXS profiles around the transition. Just below the B→C transition temperature, the SAXS peak is simple and sharp. Passing the transition temperature, two types of change were observed in the profiles. After the diffraction peak becomes diffuse, it moves to a wider angle which approximately corresponds to

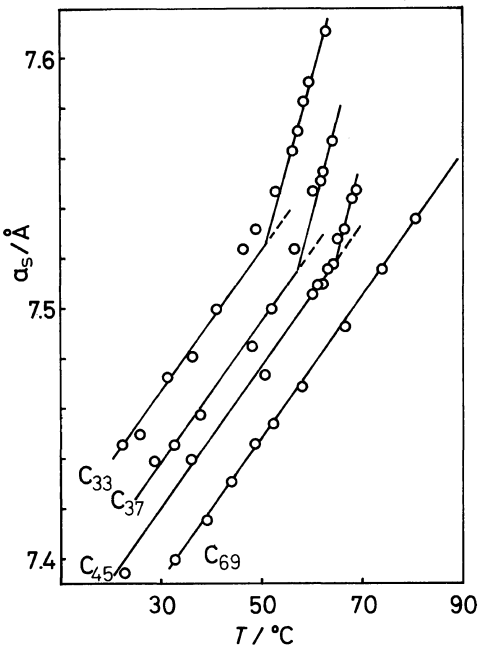

Figure 4. Temperature dependence of a_s subcell length for n-$C_{33}H_{68}$(C_{33}), n-$C_{37}H_{76}$(C_{37}), n-$C_{45}H_{92}$(C_{45}), and n-$C_{69}H_{140}$(C_{69}) crystals.

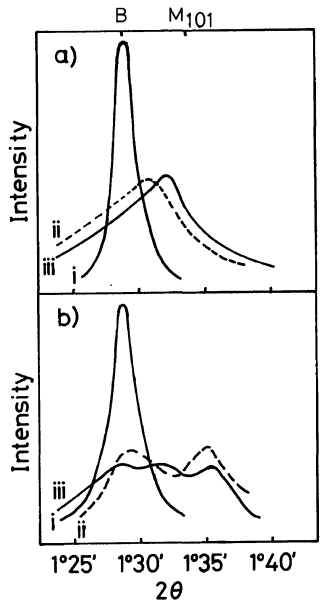

Figure 5. Two types of temperature dependence of small-angle X-ray diffraction peak observed on n-$C_{45}H_{92}$ crystals. Different modes of the temperature change (5a, and 5b) are described in the text. Measuring temperature: (a) i; 66.1, ii; 68.6, iii; 69.9°C, (b) i; 68.4, ii; 69.4, iii; 71.9°C.

the long period of M_{101} (Figure 5a). This profile did not change up to the melting. Another change is shown in Figure 5b: just above the transition temperature, the single diffraction peak changes into two peaks, and a subsequent increment of 1°C resulted in a three peak profile. The peak maxima gave long period somewhat larger than those corresponding to the orthorhombic and two monoclinic forms, M_{101} and M_{201}. This three peak profile was observed up to a temperature near the melting point.

The difference in behavior can be ascribed to the difference in heating mode of the measurements. The procedure was as follows. Before the SAXS measurement at a given temperature, which required 20 min for scanning, the sample was held for 20 min at the measuring temperature. After this the thermostat temperature was raised to the next measuring temperature. Temperature increment and heating rate to the next measuring temperature were arbitrarily selected. A larger increment in temperature and fast heating, especially around the transition temperature, resulted in the manner of change depicted in Figure 5a.

This complicated behavior of the transition raises questions about the structure of the high-temperature phase and also the kinetics of the solid-solid transition. The M_{101} structure of n-$C_{33}H_{68}$ was crystallographically determined.[2] On the other hand, SAXS measurements on higher n-alkanes, as will be shown in succeeding paragraphs, showed that for both the odd and even n-alkanes the long periods of their high-temperature phases became shorter than those of their M_{101} structures. These high-temperature structures were assigned to M_{201}, on the assumption that the oblique structure of n-alkanes has an end methyl plane indexable with simple integers.[5] It is reasonable to consider that the structure of the high-temperature phase depends on the chain length: the M_{101} for shorter chains, and the M_{201} for longer ones. For convenience, the high-temperature phases are often denoted as the phase C, despite the different structures. It seems that there is little difference in free energy for n-$C_{45}H_{92}$ between M_{101} and M_{201}, because it lies in a border region. Large increments in temperature and fast heating may induce a kinetically favorable phase

transition in crystal, *i.e.*, the M_{101} transition. One reason for the coexistence of the three phases may be that the velocity of the solid-solid transition is so small that the original and M_{101} phases are easily superheated.

In conjunction with this kinetic viewpoint, some comment is given on the motions of higher *n*-alkane molecules at high temperature. Optical observations as shown in Figure 3 suggest that the B→C transition proceeds with the general features of the phase transition—nucleation and growth. Because the direction of the chain axis is held, the transformation mechanism may consist of rotational and longitudinal jump motions, just as described generally for the molecular motion at high temperature. The difference is in that the motions for the phase transition are localized at the growth front. Furthermore, a very slow rate of the solid-solid transition can be expected from such a mechanism. It is possible that a superheated state is easily realized. When an experimental observation is made as a function of temperature passing through the transition temperature, the velocity of increasing temperature, either stepwise or continuous, may become comparable with the transition velocity. Under such circumstances, it is difficult to differentiate whether the motion is due to the transition mechanism or characteristic of the high-temperature phase. In order to reconcile the model for the molecular motion with our experimental observations, a working hypothesis is proposed that the rotational and longitudinal motions occur only as the transformation process to the high temperature phase.

The Solid-solid Phase Transitions of Higher Odd n-Alkanes

Higher odd *n*-alkanes, *n*-$C_{61}H_{124}$, *n*-$C_{65}H_{132}$, and *n*-$C_{69}H_{140}$ were synthesized. GC was not applicable for checking their purity due to their high boiling points. The GPC elution peak was simple, but it provided no information about sample purity with a sensitivity as high as the GC. The purity was estimated to be order of 99.8% based on knowledge of synthetic method for lower homologues. Odd *n*-alkanes show no complexity in crystalline form when the sample is crystallized from solution. Their stable form is only orthorhombic, differing from even *n*-alkanes. The lozenge-shaped crystals were obtained, but were thinner than those of the lower

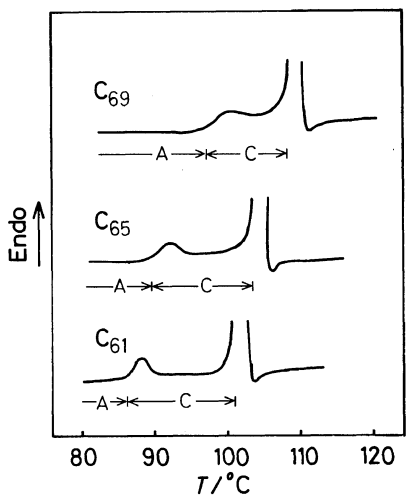

Figure 6. DSC curves of *n*-$C_{61}H_{124}(C_{61})$, *n*-$C_{65}H_{132}(C_{65})$, and *n*-$C_{69}H_{140}(C_{69})$ crystals.

homologues. The crystals consisted of two or three molecular layers. All measurements were carried out on pressed mats.

The odd *n*-alkanes studied each showed only one solid-solid phase transition below the melting (Figure 6). The transition temperature approaches the melting point with an increasing number of carbon atoms in the chain. The a_s length for *n*-$C_{69}H_{140}$ linearly increased with temperature up to the transition temperature (Figure 4). That the phase B does not exist can be concluded from the argument made in the preceding paragraph. The temperature variation of L (Figure 7a) shows that for each *n*-alkane, L is constant up to the solid-solid transition temperature, above which L continuously decreases. The constancy of L also indicates the absence of the phase B. For *n*-$C_{69}H_{140}$, the relative integrated intensity of the first-order diffraction maximum, after being normalized to the value at 40°C, is plotted against temperature in Figure 7b. An abrupt increase in the relative intensity begins at the transition temperature.

The phase notation C is used for the high-temperature phase according to the usage in the preceding paragraph. The A→C transition temperature determined from the SAXS measurements was somewhat lower than that found in the DSC curve in Figure 6. Higher alkanes suffered a greater effect of heating-rate on the solid-solid transition temperature than lower homologues did. The regular

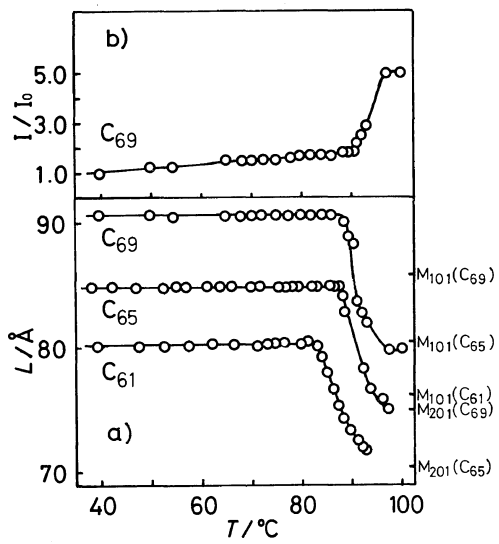

Figure 7. (a) Long periods for n-$C_{61}H_{124}(C_{61})$, n-$C_{65}H_{132}(C_{65})$, and n-$C_{69}H_{140}(C_{69})$ crystals; and (b) integrated intensity for C_{69} as functions of temperature. Calculated L of the M_{101} and the M_{201} structure for each alkane are given.

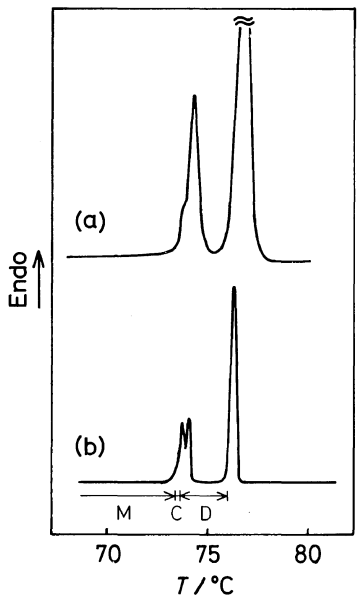

Figure 8. Effect of heating rate on peak separation of the solid-solid transitions on DSC curve of n-$C_{36}H_{74}$ crystals. Heating rate (a) 5, and (b) 0.625 K min^{-1}

striations, characteristic of oblique structures, were observed on crystals of n-$C_{69}H_{140}$ annealed at 100°C. The calculated L values as M_{101} and M_{201} for each n-alkane are shown in Figure 7. The phase C of the alkane in this range of chain length seems to have the M_{201} structure, although the observed L values are larger by about 4 Å than the calculated ones. A low degree of correlation between the molecular layers, resulting from thin plate-like crystals, may easily generate voids after the transition.

The Solid-solid Phase Transitions of Even n-Alkanes

It is well known that when crystallized from a solution, even n-alkanes sometime assume the monoclinic form and in other cases the orthorhombic form; the former is a stable modification. This complexity may be ascribed to kinetic factors in the crystallization as well as a very small difference in the free energies of the two forms. In addition, impurities generally lead to the orthorhombic form. The shorter even n-alkanes of the highest purity, n-$C_{32}H_{66}$ and n-$C_{36}H_{74}$, always crystallized in the monoclinic form. This form is denoted by M_{011} according to the Sullivan-Weeks' notation. It is desirable to recognize definitely the difference between the monoclinic structures, M_{011} and M_{h01} (usually $h=1$ or 2). Staggering of the chain molecules occures in the $(010)_s$ plane for the former and in the $(100)_s$ plane for the latter, respectively. The former can be observed only at room temperature, and the latter at higher temperature. To distinguish the structural difference, it is pertinent to use the following terms, the low-temperature monoclinic form and the high-temperature one for M_{011} and M_{h01}.

In Figure 8 are depicted the DSC curves of n-$C_{36}H_{74}$ (M_{011}) obtained at the heating rate of 0.625 and 5 K min^{-1}. The slow heating rate allows a good resolution of a small endothermic peak before the rotator transition. This confirms that monoclinic n-$C_{36}H_{74}$ transforms into the rotator phase through an intermediate form, which exists in a very narrow temperature range when the sample is quite pure.[1,18] For n-$C_{32}H_{66}$ (M_{011}), the direct transition of the monoclinic to the rotator phase was observed on DSC even at the lowest rate of heating, 0.625 K min^{-1}.

There still is uncertainty about the structure of the intermediate phase of n-$C_{36}H_{74}$. X-ray studies[16,19] on samples which do not seem to have been pure enough indicated that the intermediate phase is orthorhombic, but a thermodynamic

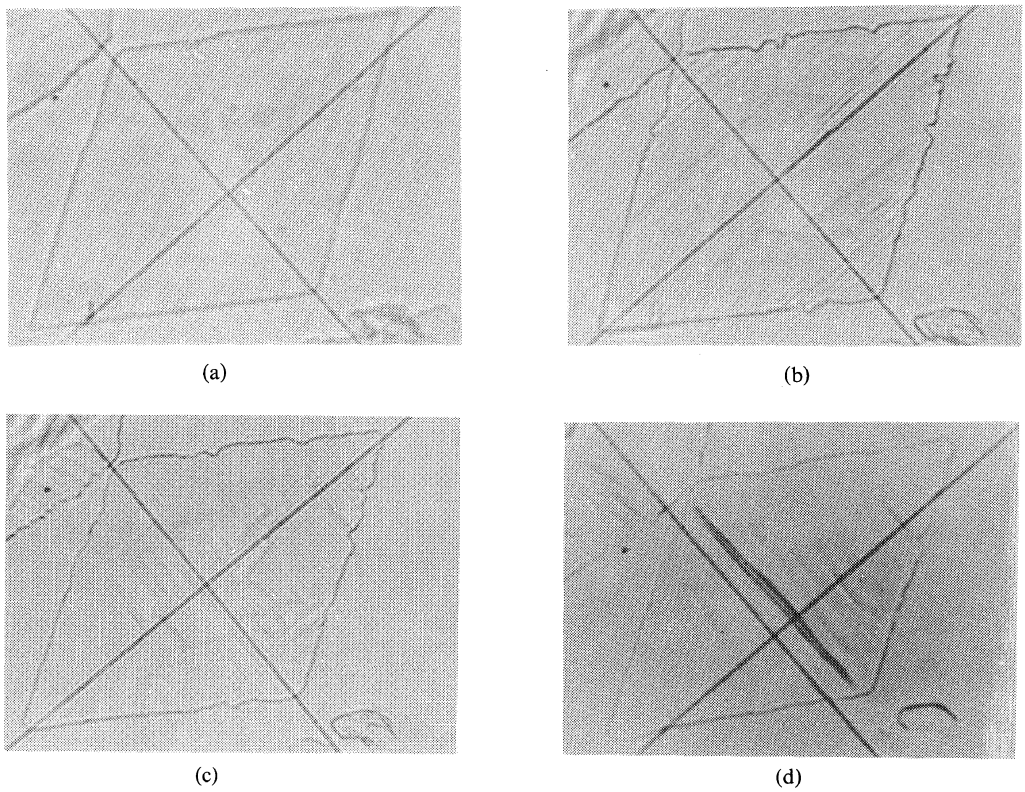

Figure 9. Photomicrographs of n-$C_{36}H_{74}$ crystal in monoclinic form at various temperature regions: (a) at room temperature; (b) at an initial stage of the phase C region; (c) just after the *b* stage; (d) at the phase D region.

study on a pure sample[18] disagreed with this conclusion.

Morphological change of n-$C_{36}H_{74}$ (M_{011}) crystals was observed with an optical microscope, continuously heating the sample. Its feature was the appearance of the striations parallel to the a_s axis of a crystal. These striations immediately disappeared before the b_s-striations were observed (Figure 9). Because of the difficulty of fine temperature control, it was impossible to correlate this observation with the details of the phase transition. The rotator phases of n-$C_{32}H_{66}$ and n-$C_{36}H_{74}$ were found to have long periods calculated from the M_{101} structure. It is reasonable to suppose that the intermediate phase of n-$C_{36}H_{74}$ has an identical L with the rotator phase. Hence, the intermediate phase is concluded to be high-temperature monoclinic. This conclusion may be extended to n-$C_{32}H_{66}$: The monoclinic crystal transforms to the M_{101} just below the rotator transition, even if the DSC peak can not be resolved. The b_s-striations can be ascribed to the development of the high-temperature monoclinic form, as is the case with odd n-alkanes. If the progressive slipping mechanism of the chain molecules works at the growth front of the solid-solid transition, the M_{011} structure should transform into the M_{h01} *via* the vertical structure as an activated state which corresponds to the appearance of the a_s-striations. Although the detailed mechanism for this is still open to question, this observation gives rise to additional problems regarding the mechanism of solid-solid transition of long chain molecules.

With increasing chain length it became difficult to allow even n-alkanes to grow single crystalline forms by solution crystallization. Table I lists the experimental results obtained when n-$C_{48}H_{98}$ was allowed to crystallize under various conditions. The ratio of both crystalline modifications in a sample was estimated from the ratio of the intensities of

Table I. Effect of crystallization conditions on ratio of orthorhombic to monoclinic modification for n-$C_{48}H_{98}$

Solvent	Concentration / %	Cooling	Ratio of orthorhombic modification / %
Hexane	5	Rapid	100
Isoamyl acetate	0.5	Slow[a]	88
Isoamyl acetate	0.25	Slow	78
Benzene	0.5	Slow	23
Benzene	0.25	Slow	30
Hexane	0.5	Slow	12
Hexane[b]	0.5	Slow	0

[a] About 1 K h^{-1}.
[b] The crystallization was carried out in a Teflon vessel.

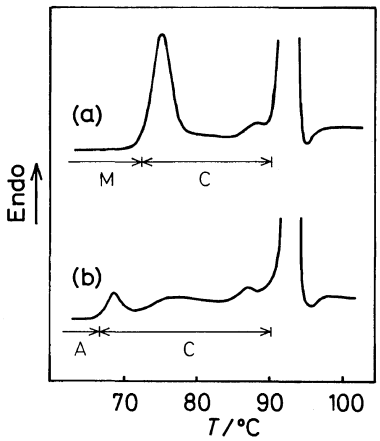

Figure 10. DSC curves of n-$C_{48}H_{98}$; (a) in monoclinic and (b) in orthorhombic modification.

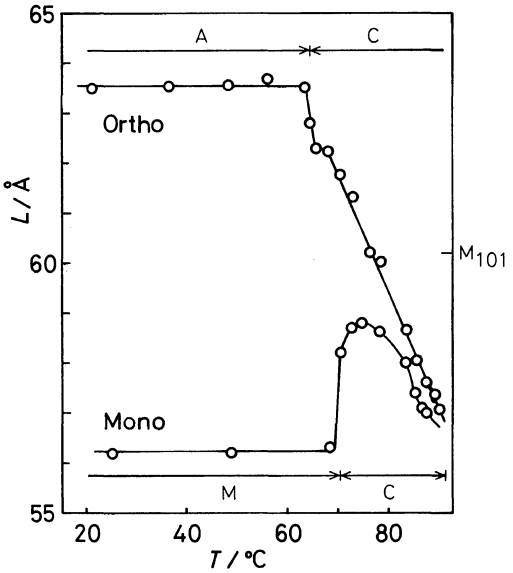

Figure 11. Temperature dependence of long periods of n-$C_{48}H_{98}$ crystals of two modifications. Abbreviations in the figure mean monoclinic and orthorhombic modification, respectively.

their SAXS peaks. Pure monoclinic crystals were obtained only when a hexane solution was cooled slowly (about 1 K h^{-1}) in a Teflon container, which prevented nucleation on the wall of the container. Quenching the solution gave pure orthorhombic crystals. Higher temperature crystallization also seemed to give rise to the orthorhombic form.

The monoclinic and orthorhombic n-$C_{48}H_{98}$ showed DSC curves in Figure 10, having the characteristic feature of the solid-solid transition. Figure 11 depicts the temperature variation of the long period for both forms. The observed values of L for both forms at room temperature are in good agreement with those calculated by the relation for the M_{011},[17]

$$L = 1.106n + 3.93 \quad (\text{in Å}) \qquad (2)$$

and by eq 1 for the orthorhombic form. The temperatures at which L changes are correlated with those determined from the DSC curves. The difference in the transition temperatures of the different modifications indicates that the monoclinic form is stable. The change of L in the high-temperature phase (Figure 11) suggests that the M_{101} structure at

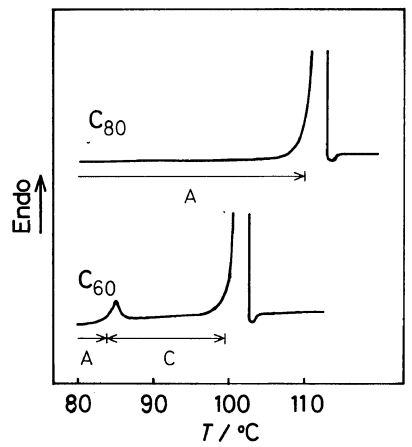

Figure 12. DSC curves of higher even *n*-alkanes: *n*-$C_{60}H_{122}(C_{60})$ and *n*-$C_{80}H_{162}(C_{80})$ crystals.

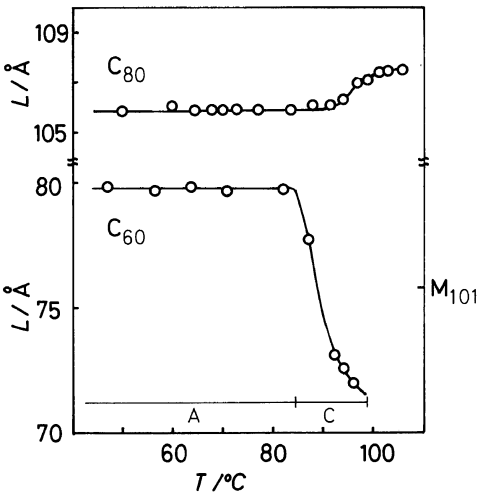

Figure 13. Long periods of *n*-$C_{60}H_{122}(C_{60})$ and *n*-$C_{80}H_{162}(C_{80})$ crystals as functions of temperature.

first appears and then transforms to the M_{201}. It may be possible to correlate this transformation to the small peaks observed just below the melting on the DSC curves in Figure 10. Passing through the high-temperature phase gives to the identical melting point for *n*-$C_{48}H_{98}$, independently of its low-temperature modifications. The behavior of the high-temperature phase was complex. Sometime the orthorhombic *n*-$C_{48}H_{98}$ showed the coexistence of two types of structure, perhaps the original orthorhombic and the M_{201} structure, over the region of the high-temperature phase, as in the case of *n*-$C_{45}H_{92}$. In order to elucidate their complicated behavior, it will be necessary to carry out kinetical experiments, taking into account of the effect of the chain length.

A further increase in the number of carbon atoms in even *n*-alkane gave only the orthorhombic crystal from its solution crystallization. The DSC curves for *n*-$C_{60}H_{122}$ and *n*-$C_{80}H_{162}$ are given in Figure 12, and the temperature change of their L in Figure 13. Comparison of thermal behavior between *n*-$C_{60}H_{122}$ and *n*-$C_{61}H_{124}$, both in the orthorhombic form, indicates that the even-odd effect of the number of carbon atoms disappears not only in the melting point but in the solid-solid transition temperature for higher *n*-alkanes. Melting of *n*-$C_{60}H_{122}$ occurs after passing through the high-temperature monoclinic phase. The DSC curve of *n*-$C_{80}H_{162}$, however, reveals no indication of the solid-solid transition before the melting. Thermal behavior of the long period of this compound differs from that of the other *n*-alkanes mentioned above. The L is constant up to about 90°C, above which it gradually approaches a value as high as about 1.2 Å. The highest measuring temperature was about 3°C lower than the melting point. This behavior is also different from that reported for *n*-alkanes by other researchers.[6,9] Sullivan and Weeks[6] reported that solution-crystallized *n*-$C_{94}H_{190}$ in the orthorhombic form showed no structural change up to 65°C, but upon heating to 108°C (5°C lower than the melting point) it transformed to the high-temperature monoclinic form. Khoury[27] also reported that melt-crystallized *n*-$C_{94}H_{190}$ is high-temperature monoclinic. What is the cause for the difference in the appearance of the high-temperature phase between *n*-$C_{94}H_{190}$ and *n*-$C_{80}H_{162}$? The sample purity seems to play an important role for the difference. There is uncertainty about the determination of the purity. Davis *et al.*[28] estimated the purity of *n*-$C_{94}H_{190}$ samples for their study to be 90% by a thermal method. If the *n*-$C_{94}H_{190}$ samples used by the members of the National Bureau of Standards were from the same source, the difference may be ascribed to impurity effects. As stated in the EXPERIMENTAL section, there was the possibility that Reinhard–Dixon's method might give *n*-$C_{84}H_{170}$ as an impurity in the sample of *n*-$C_{94}H_{190}$. On the other hand, our sample of *n*-$C_{80}H_{170}$ showed a single elution peak on the GPC curve. However, this does not guarantee the

Table II. Transition temperatures of the *n*-alkanes[a] (in °C)

Number of carbon atoms	A→B	B→C	A→C	M→C	C→D	Melting
32				(66.4)[b]	(66.4)[b]	70.4
33	53.5	64.4			67.6	71.1
36				70.9	74.0	75.9
37	56.5	65.8			76.3	77.2
45	62.0	68.9				87.2
48			64.1			90.5
48				71.7		90.5
60			81.9			99.1
61			84.0			100.3
65			87.5			102.1
69			89.4			104.7
80						108.0

[a] The indicated phase transition at the top of a column is described in the text.
[b] Although two transitions could not be resolved, their existence has been proposed. See text.

high purity, because GPC is not very sensitive. Heitz *et al.*[9] reported that L of n-$C_{70}H_{142}$ began to decrease between 73° and 81°C and became about 10 Å shorter just below the melting point. When compared with our data on n-$C_{69}H_{140}$, this temperature for the onset of decrease in L is too low. Moreover, they reported no thermal indication corresponding to this transition temperature. These facts indicate that their n-$C_{70}H_{142}$ was not pure enough. In order to elucidate clearly the thermal behavior of higher *n*-alkanes ($n \geq 80$) of high purity, we have to find a better synthetic route to obtain them.

Relationships between Transition Temperatures and the Number of Carbon Atoms in an n-Alkane Molecule

In Table II are summarized the solid-solid transition temperatures, along with the melting points and the rotator transition points for the *n*-alkanes studied in this work. The phase notation system used here is as follows. For odd *n*-alkanes the notation according to the German group is adopted, that is, A, B, C, and D in order of increasing temperature. The symbol D represents the rotator phase not only of odd *n*-alkanes but of even ones too. For even *n*-alkanes in low-temperature forms, the symbol A is used for the orthorhombic and the symbol M for the low-temperature monoclinic modification (M_{011}). The symbol C is used to designate the high-temperature monoclinic modifications which have not connection with their detailed structures.

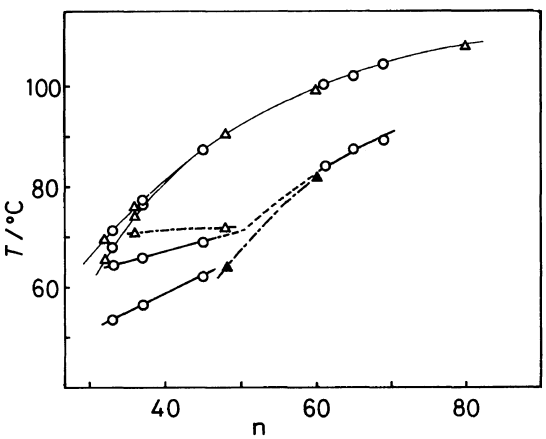

Figure 14. Temperatures of various types of transition *vs.* the number of carbon atoms per molecule: fine solid lines for melting and rotator transition; solid lines for solid-solid transition lines of odd *n*-alkanes; dashed lines for solid-solid transition lines of even *n*-alkanes.

The solid-solid transition temperatures listed in Table II are those determined by SAXS and WAXS

measurements. These transition temperatures are free from heating rate effects. However, some data are less accurate, since the temperature increment around the transition was not so small. For the melting point and the rotator transition point, the values determined by the DSC method are used.

These transition temperatures are plotted against the number of carbon n in Figure 14. The transition lines A→B, B→C, and A→C for odd *n*-alkanes are drawn by solid curves, and the M→C and the A→C lines for even *n*-alkanes by dashed lines. We cannot describe the general behavior of the solid-solid transition lines because the situation is complicated and the number of data point is still insufficient.

The upward trend of the A→C transition line over a wide range of chain lengths has an important meaning in discussing the thermal behavior of *n*-alkanes in conjunction with that of polymeric crystals. From the standpoint of the molecular motions, the transition line indicates at least the onset of an uncoupled rotational and longitudinal motion or the coupled motion—flip-flop motion irrespective of the kinetic or the intrinsic viewpoint on the molecular motions. The onset temperature increases up to about 90°C with an increase in chain length. This finding differs from that structural changes in crystalline higher *n*-alkanes are said to occur at about 70°C. It should be emphasized that homologous impurities in crystalline *n*-alkane have an appreciable effect on the transition behavior.

It is reasonable to consider that the A→C transition line of odd *n*-alkanes agrees with that of even *n*-alkane. It is, however, uncertain whether the A→C line intersects with the melting line at some higher chain length, as stated in detail in the preceding paragraph. Broadhurst[17] proposed a transition line for the monoclinic-to-orthorhombic transformation for even *n*-alkanes with n higher than 34, on the basis of a limited amount of information. Since the modification he designated as the orthorhombic form is high-temperature monoclinic, his reported transition line must be referred to as the M→C transition line. The M→C line fitting our two data points is shown by the dot-dashed line. If this line could be linearly extrapolated to longer chains, it would intersect with the A→C line for even *n*-alkanes. This implies that the stable form at room temperature changes from the monoclinic to the orthorhombic form of longer chains. Another interesting point is concerned with whether the B phase region which exists only for odd *n*-alkanes is closed or not.

CONCLUSIONS

Higher *n*-alkanes from n-$C_{32}H_{66}$ to n-$C_{69}H_{140}$ were synthesized, with special attention paid to their purity. The purity of these compounds was at least 99%. The thermal behavior of the *n*-alkanes was examined by DSC, WAXS, and SAXS measurements. The features of the solid-solid transitions of the *n*-alkanes are summarized as follows:

a) The high-temperature phase appears before the melting or the transition to the rotator phase, irrespective of whether the number of carbon atoms in the chain is odd or even. The difference in the room-temperature modification for n-$C_{48}H_{98}$ also has no effect on this situation.

b) The high-temperature phase is high-temperature monoclinic: the M_{101} structure for shorter chains and the M_{201} for longer chains.

c) Solution-grown crystals clearly show a thermal indication of the first order transition, corresponding to the structural change.

d) The solid-solid transition shows a remarkable irreversibility, and its rate is slow.

e) The odd *n*-alkanes from n-$C_{33}H_{68}$ to n-$C_{45}H_{92}$ have another solid-solid transition, in addition to that described above.

Along with these experimental facts, a working hypothesis on the molecular motions at high temperature is proposed: the rotational and longitudinal motions take place only at the phase transition.

REFERENCES

1. A. A. Schaerer, C. J. Busso, A. E. Smith, and L. B. Skinner, *J. Am. Chem. Soc.*, **77**, 2017 (1955).
2. W. Piesczek, G. Strobl, and K. Malzahn, *Acta Crystallogr., Sect. B*, **30**, 1278 (1974).
3. R. K. Sullivan, *J. Res. Natl. Bur. Stand.*, **78A**, 129 (1974).
4. P. R. Templin, *Ind. Eng. Chem.*, **48**, 154 (1956).
5. A. Keller, *Phil. Mag.*, **6**, 329 (1961).
6. T. K. Sullivan and J. J. Weeks, *J. Res. Natl. Bur. Stand.*, **74A**, 203 (1970).
7. B. Wunderlich, "Macromolecular Physics," Vol. 3, Academic Press Inc., New York, 1980, p 234.

8. D. D. Pope and A. Keller, *J. Polym. Sci., Polym. Phys. Ed.*, **14**, 821 (1976).
9. W. Heitz, Th. Wirth, T. Peters, G. Strobl, and E. W. Fischer, *Makromol. Chem.*, **162**, 63 (1972).
10. G. Strobl, B. Ewen, E. W. Fischer, and W. Piesczek, *J. Chem. Phys.*, **61**, 5257 (1974).
11. B. Ewen, E. W. Fischer, W. Piesczek, and G. Strobl, *J. Chem. Phys.*, **61**, 5265 (1974).
12. G. R. Strobl, *Colloid Polym. Sci.*, **254**, 170 (1976).
13. B. Ewen and D. Richter, *J. Chem. Phys.*, **69**, 2954 (1978).
14. G. R. Strobl, *J. Polym. Sci., Polym. Symp.*, **No. 59**, 121 (1977).
15. B. Ewen, G. R. Strobl, and D. Richter, *Faraday Discuss. Chem. Soc.*, **69**, 19 (1980).
16. S. Barbezat-Debreuil, *Comptes Rendus*, **246**, 2907 (1958).
17. M. G. Broadhurst, *J. Res. Natl. Bur. Stand.*, **66A**, 241 (1962).
18. C. M. L. Atkinson and M. J. Richardson, *Trans. Faraday Soc.*, **65**, 1749 (1969).
19. A. Kawaguchi, *Bull. Inst. Chem. Res. Kyoto Univ.*, **56**, 68 (1978).
20. S. Hünig, H. J. Buysh, H. Hoch, and W. Lendle, *Chem. Ber.*, **100**, 3996 (1967).
21. G. Ställberg, S. Ställberg-Stenhagen, and E. Stenhagen, *Acta Chem. Scand.*, **6**, 313 (1952).
22. R. R. Reinhard and J. A. Dixon, *J. Org. Chem.*, **30**, 1450 (1965).
23. T. Oyama, K. Takamizawa, and Y. Ogawa, *Kobunshi Ronbunshu*, **37**, 711 (1980).
24. Y. Ogawa, Doctorial thesis, Kyushu University, 1981.
25. W. H. Carothers, J. W. Hill, J. E. Kirby, and R. A. Jacobson, *J. Am. Chem. Soc.*, **52**, 5279 (1930).
26. K. Takamizawa, Y. Sasaki, K. Kono, and Y. Urabe, *Rep. Prog. Polym. Phys. Jpn.*, **19**, 285 (1976).
27. F. Khoury, *J. Appl. Phys.*, **34**, 73 (1963).
28. G. T. Davis, J. J. Weeks, G. M. Martin, and R. K. Eby, *J. Appl. Phys.*, **45**, 4175 (1974).
29. H. G. Olf and A. Peterlin, *J. Polym. Sci., A-2*, **8**, 753 (1970).
30. H. G. Olf and A. Peterlin, *J. Polym. Sci., A-2*, **8**, 791 (1970).